

## Alkali halide decomposition and desorption by photons—the role of excited point defects and surface topographies

This article has been downloaded from IOPscience. Please scroll down to see the full text article.

2006 J. Phys.: Condens. Matter 18 S1547

(<http://iopscience.iop.org/0953-8984/18/30/S09>)

View [the table of contents for this issue](#), or go to the [journal homepage](#) for more

Download details:

IP Address: 129.252.86.83

The article was downloaded on 28/05/2010 at 12:29

Please note that [terms and conditions apply](#).

# Alkali halide decomposition and desorption by photons—the role of excited point defects and surface topographies

Marek Szymonski, Anna Droba, Maria Goryl, Jacek J Kolodziej and Franciszek Krok

Research Centre for Nanometer-Scale Science and Advanced Materials (NANOSAM), Institute of Physics, Jagiellonian University, ulica Reymonta 4, 30-059 Kraków, Poland

Received 1 February 2006, in final form 14 April 2006

Published 14 July 2006

Online at [stacks.iop.org/JPhysCM/18/S1547](http://stacks.iop.org/JPhysCM/18/S1547)

## Abstract

Our recent work on photon-stimulated desorption of alkali halide surfaces has been reviewed. Most of the experimental data are presented for the first time. This new material is supplemented with two examples of our work published previously (see Szymonski *et al* 1996 *Surf. Sci.* **363** 229; 2002 *Acta Phys. Pol.* **33** 2237). The results are discussed and compared with relevant experimental and theoretical work by other authors. In particular, we focus on two aspects of the studies: high resolution AFM imaging of desorbed surfaces, and measurements of mass selected fluxes of the desorbing atoms. It is found that, at initial stages of the UV-photon stimulated desorption, the process is occurring in a 'layer-by-layer' mode as a result of growth and linking of monatomic pits on the surface. This results in periodic changes of surface topography from atomically flat to rough with a period equal to the time needed for desorption of 1 ML. Such periodic changes of the surface topography affect the efficiency of the desorption and result in oscillatory dependence of the emitted particle yields versus photon fluence. Careful analysis of the yields reveals that during irradiation there is a substantial number of stable ground state F-centres accumulated under the surface. The number of accumulated defects is changing periodically with the photon fluence in anti-correlation with the desorption yields. Based on the mentioned results, we argue that the production of F-centres and their interaction with the surface are, in fact, the limiting factor for PSD. To test the validity of this statement a series of desorption experiments for the crystal co-irradiated with visible light (with a wavelength corresponding to the F-centre absorption band) and UV photons have been performed. A dramatic increase in the desorption yield, as well as pronounced changes in the surface erosion process, have been found.

## 1. Introduction

The phenomenon of desorption induced by electronic transitions (DIET), i.e. emission of surface particles due to the inelastic interaction with ionizing radiation, has been investigated for several decades [1–4]. For the case of ionic insulators, atomic constituents of the irradiated crystal are emitted as desorbed species. Although details depend on a particular crystal and the experimental conditions, in general, neutral atoms are desorbed ( $\sim 80\text{--}90\%$ ), with admixture of molecules ( $\sim 10\text{--}20\%$ ) and a small fraction of ions ( $\sim 10^{-3}\text{--}10^{-5}\%$ ) [2].

Translational energy distributions of particles electron-desorbed from alkali halides are best known [5–7], and they consist of a thermal (Maxwellian) component for metal neutrals (i.e. alkali atoms), and two components, thermal and hyper-thermal ones, for halogen atoms. Recently, energy distributions of halogen atoms desorbed due to UV-laser irradiation have been studied [8–13], and predominantly the hyper-thermal component was found for close-to-threshold (the fundamental surface exciton) excitations. Both thermal and non-thermal velocity components have been found for excitations with energies higher than the bandgap energy.

It is known that both photons and energetic electrons can excite alkali halide crystals, creating conduction band electrons and valence band holes. Depending on the relative energy, these primary excitation products may be quite mobile, migrate independently in the crystal and eventually thermalize to form bound pairs, so called ‘self-trapped excitons’. Creation of free conduction electron and valence holes occurs predominantly for electron bombardment, whereas direct formation of excitons could dominate for irradiation with low energy photons (within the energy band of either bulk, or surface exciton). Most of the experimental observations so far yielded qualitatively similar results for both electron stimulated desorption (ESD) and photon stimulated desorption (PSD). There are several reports, however, which emphasize important differences between the two excitation paths [13–15]; therefore, a thorough review and detailed discussion of these data are necessary in order to achieve satisfactory understanding of the phenomena of photon energy conversion into excitation, the excitation diffusion and emission of particles from surfaces.

Research on photon-stimulated desorption of ionic surfaces can be discussed along various aspects related to the primary excitation process:

- threshold excitation phenomena (excitation function, surface versus bulk excitons, surface precursor states for desorption, etc),
- valence excitation (exciton formation and decay, electron–hole pairs, Frenkel defects, defect diffusion, surface phenomena, surface topography modification, yield oscillations, recombination luminescence),
- core excitation (absorption function, adsorption edge phenomena, Auger processes, Knotek–Feibelman mechanism, secondary electron cascades, electron–hole plasma density),
- co-excitation with light (visible light absorption, F-centre diffusion role),
- desorption mechanisms (theory, experimental data interpretation, etc).

In our overview we will focus on the first two and the last two items on the list. The core excitation photodesorption will not be discussed in this work. The bulk of experimental data presented in this paper (displayed in figures 2–6 and 8–10) represents new results which have not been published elsewhere.

## 2. Experimental methods

The experiments described in this work were carried out in a UHV chamber with a base pressure of the order of  $2 \times 10^{-8}$  Pa. Alkali halide crystals were cleaved in air and subsequently mounted on a sample holder of which the temperature could be changed between room temperature and 700 K as measured by a thermocouple. Desorption and surface modification was stimulated either by a UV light generated by a deuterium lamp (4–6 eV), or a UV OPA pulsed laser with photon energy of 5.81 eV (laser facility of the Vanderbilt University, Nashville, TN, USA). The signals of emitted atoms were measured by a quadrupole mass spectrometer (QMS) for both crystal components, or alternatively by a surface ionization detector for alkali atom detection. The surface ionizer consisted of a rhenium filament heated by electric current to the temperature of about 1400 K and a channeltron. Velocity spectra of desorbed particles were measured by means of a time-of-flight spectroscopy. The primary photon beam from the deuterium lamp was mechanically modulated into pulses of 0.05 ms width and separated by time intervals of 5 ms. After a flight path of 9.5 cm, the particles were ionized in an electron impact ionizer and mass selected in QMS. The white light for F-centre band excitation was provided by a 150 W halogen bulb. Whenever appropriate the wavelength of light was chosen by use of interference filters of  $\sim 7$ –8 nm bandwidth. In addition, some co-excitation experiments were performed with second harmonic radiation of the Nd:YAG pulsed laser ( $\lambda = 532$  nm).

Dynamic (non-contact) force microscopy (DFM) was used to image irradiated surfaces. In DFM a sharp tip is mounted on a cantilever which is driven in its resonant frequency just over the sample surface. The surface topography is measured by adjusting the cantilever position with respect to the surface in order to keep its frequency constant, i.e. by mapping the surface of constant tip–surface interaction. A PSI VP2 microscope with Nanosurf easyPLL demodulator was used in the experiment. The cantilever resonant frequency was approximately 150 kHz and the applied de-tunings were between 40 and 120 Hz.

Rapid annealing of the crystals to 600 K in time less than 1 min was found to be an efficient way of removing surface modification introduced by UV light. That procedure was applied routinely before every irradiation in order to assure the same starting experimental conditions.

## 3. Desorption by excitation at threshold energies

Photon-stimulated desorption from KI at threshold energies (5–10 eV) has been studied by Brinciotti *et al* [16, 17]. In more recent works [18, 19], the relative desorption yields and angular distributions of alkali and halogen atoms desorbed from (100) surfaces of KI and RbI were measured as a function of the synchrotron radiation energy. The desorption data were compared with the surface reflectivity spectrum measured in parallel with PSD signals. The dependence of the I atom desorption yield for the RbI(001) crystal as a function of the synchrotron radiation energy is reproduced from [18] in figure 1. In order to correlate the onset of the desorption yield with the spectral dependence of the exciton formation, the surface reflectivity curves are displayed in the same figure. It is seen that the onset of desorption agrees well with the energy required for excitation of the lowest exciton state. The same observation was made for the KI crystal [18, 19]. Recent PSD experiments by Hess *et al* [8–13] have been performed with highly selective laser excitation. That high selectivity of the excitation source enabled the authors to distinguish between the desorption onset corresponding to the Urbach tail of the surface exciton excitation function and the higher-energy features corresponding to bulk exciton excitation and electron–hole pair creation. It is believed that a non-radiative decay of the surface exciton results in non-thermal halogen emission [2, 4, 13]. Based on the

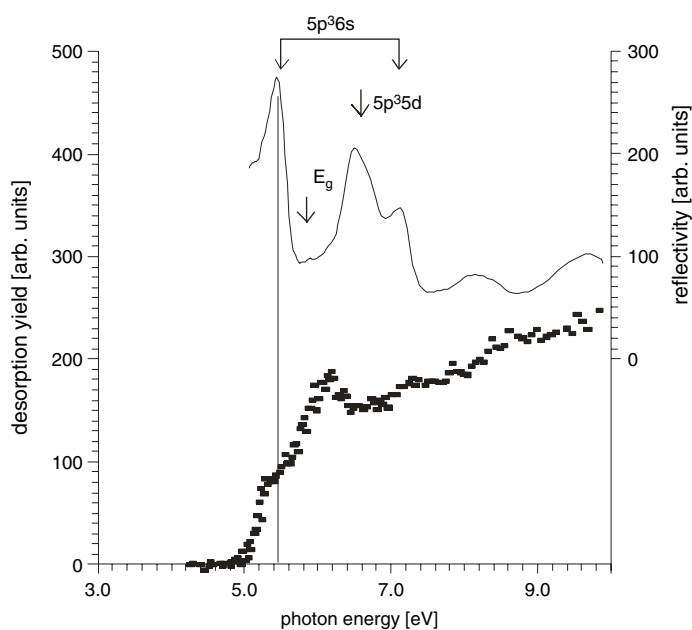


**Figure 1.** Dependence of the desorption yield of I atoms emitted from RbI on the synchrotron radiation energy. The solid curve in the upper part of the figure represents the surface reflectivity spectrum measured in the same experiment. Reproduced from [18].

velocity distribution measurements of laser desorbed non-thermal halogen atoms, Hess *et al* [11, 12] have determined the excitation energies required for creation of the surface excitons. Since the expected surface exciton energy shifts relative to the bulk exciton energy for RbI and KI are rather small ( $\leq 0.2$  eV [13]), they could not be resolved in much less selective experiments using synchrotron radiation [18, 19]. For the same reason we would not be able to distinguish between the surface exciton excitation and the bulk one using a deuterium lamp as the excitation source. This is consistent with our time-of-flight distribution measurements for UV-photon stimulated desorption of RbI and KI. The distributions were obtained with a set-up using the mechanical chopper for photon beam modulation and the deuterium lamp as the source of UV photons with energies up to 6 eV. The time-of-flight distributions for both alkali and halogen desorption components are shown in figures 2(a) and (b). It is seen that the halogen atom velocity spectrum (figure 2(a)) consists of two components (broad thermal and narrow hyper-thermal distributions), indicating that both excitation paths, initiated either by the surface exciton or the bulk one, should be considered in the model describing PSD of alkali halides. Moreover, the alkali atom velocities (figure 2(b)) are exclusively thermal (Maxwellian), characterized by the macroscopic surface temperature, which could be measured with a thermocouple (see also figure 10). More detailed discussion of PSD mechanisms is given in section 4.

Angular characteristics of atoms desorbed from alkali iodides due to x-ray irradiation have been measured by the same authors [18]. It was found that both desorption components have essentially the same angular characteristics, which is in contrast to several ESD experiments [2, 7]. In this last case, the halogen component angular distribution could be significantly forward peaked (along the  $\langle 001 \rangle$  axis), whereas the alkali atoms are emitted with cosine-like angular distribution.

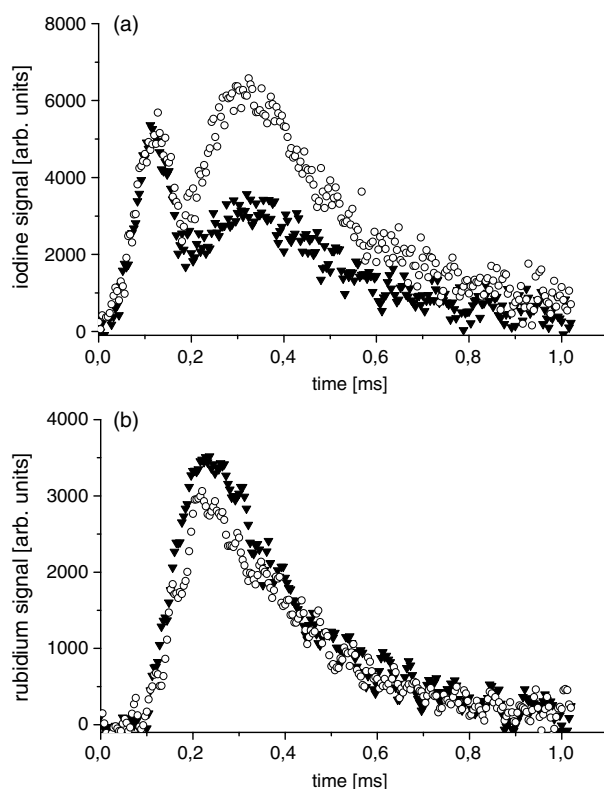


**Figure 2.** Time-of-flight distributions of atoms desorbed from (001) RbI with UV photons (deuterium lamp). (a) Halogen distributions obtained with (open circles) and without (full triangles) co-excitation by visible light. A dramatic increase of the thermal halogen component is clearly visible. The sample temperature was 60 °C. (b) Rubidium distributions obtained with (open circles) and without (full triangles) co-excitation with visible light. The shape of both distributions is preserved but the intensity of the Rb signal is lower for 'light-on' conditions. The spectra were registered at the sample temperature of 120 °C for better signal to noise ratio. For details see the text.

Hoeche *et al* [21, 22] has found that 'layer-by-layer' desorption occurred for a UV-irradiated NaCl single crystal. The authors have used He atom scattering as a tool to monitor NaCl(001) surface desorption due to UV photons generated by a deuterium lamp. Characteristic oscillations of the scattered He intensity were found, indicating the 'layer-by-layer' mode of the desorption. Furthermore, it was found that such a mode of erosion occurred in a wide range of the crystal temperatures (273–493 K). However, the mass spectrometric measurements of the desorption signal performed in the same work did not indicate any dependence of the desorption yield on the surface topography. In our more recent work the dynamic force microscopy has been used for imaging surfaces desorbed under similar experimental conditions (UV deuterium lamp excitation, the same sample temperature range). For monitoring of the desorption signals a quadrupole mass spectrometer (QMS), as well as a sensitive surface ionization detector for the alkali atoms, were used [23]. The measurements confirmed the previous findings that the desorption occurs in a layer-by-layer mode. Furthermore, high resolution DFM imaging could directly visualize the progress of the desorption process as it proceeds by creation of two-dimensional pits in the first surface

layer, then growth and coalescence of the pits transforming the surface topography from atomically flat, through the roughest stage, in which on average  $\frac{1}{2}$  of the surface monolayer is removed, to flat again for a complete monolayer removal. Such two-dimensional erosion of the surface is continued with periodic changes of the surface topography until the statistical de-coherence terminates overall periodicity of the change. In figure 3 the sequence of non-contact AFM images of UV-desorbed RbI surfaces is presented. The images were taken after various irradiation times representing selected values from the range used in separate QMS measurements of the desorption yield (see figure 4). A gradual evolution of the surface topography with increasing time of irradiation is clearly visible. A number of rectangular pits of monolayer depth with edges oriented along the main crystallographic directions of the (001) plane can be seen on the irradiated surfaces. With increasing time of irradiation, the pits grow and join together, gradually exposing the next surface plane. Large differences in the density of low-coordinated surface atoms (at pit steps, edges and corners) for various images from figure 3 are clearly visible.

Let us compare varying surface topographies of the UV-irradiated RbI crystal, as seen in AFM images, with clearly visible PSD yield oscillations as a function of irradiation time shown in figure 4. The irradiation conditions for QMS measurements from figure 4 (see the dependence for  $T = 100^\circ\text{C}$ ) were strictly the same as the ones used for obtaining surface topographies from figure 3. Apparently, the Rb desorption signal is correlated with the step density on the surface. The maximum efficiency of the process occurs for the surface, where islands of monatomic height account for  $\sim 50\%$  of the surface area (figure 3(d)). The minimum efficiency of the desorption process is observed for a flat surface with a few small pits of monatomic depth (figure 3(f)). It is seen that one period of oscillations corresponds to removal of a single monolayer. Generally, it can be concluded that the varying number of low-coordinated surface atoms is causing pronounced modulation of the desorption yield. Similarly to ESD experiments reported earlier [24–26], the oscillatory dependence in figure 4 is damped and it disappears after a certain number of cycles. This is due to the fact that some pits in the deeper layer have been created before the upper one is completely removed, cf. figures 3(f) and (g). This is a statistical process and after several cycles the well defined periodicity of the surface topography changes is lost; as a result, the oscillations in desorption efficiency are no longer observed [24, 25]. Since AFM images have been measured ‘post mortem’, i.e. several hours after the irradiation, a possibility of healing of the radiation damage inside the pits due to thermal diffusion could not be excluded based on AFM analysis alone. However, varying topography of the irradiated surface is closely correlated (in fact a 1:1 correlation is seen for removal of the first few monolayers) to variations of the desorption yield displayed in figure 4.

It is important to note that the yield oscillations are visible for both desorption components, i.e. for alkali and halogen atoms as seen in figures 4 and 5. Since the average UV light absorption coefficient for RbI at 400 K can be evaluated as equal to  $3 \times 10^5 \text{ cm}^{-1}$  [27], we could assume that most of the primary photon energy is deposited down to the depth of 60 nm, which is similar to the penetration depth of 1 keV electrons [28]. Similar desorption yield oscillations have been found previously for electron irradiated alkali halides [24, 25]. This strongly indicates that the effect of surface topography is not dependent on the primary excitation details but it is rather affecting the yield in later stages of the process when diffusion and/or surface recombination of the secondary excitation products take place.

The analysis of the oscillatory dependence of the desorbing atom fluxes on the irradiation time may be used for estimation of the desorption rate. Since removal of a single monolayer corresponds to one full period of the oscillation, we could calculate the desorption yield even in absolute units, providing that we know the accurate number of impinging photons per irradiated



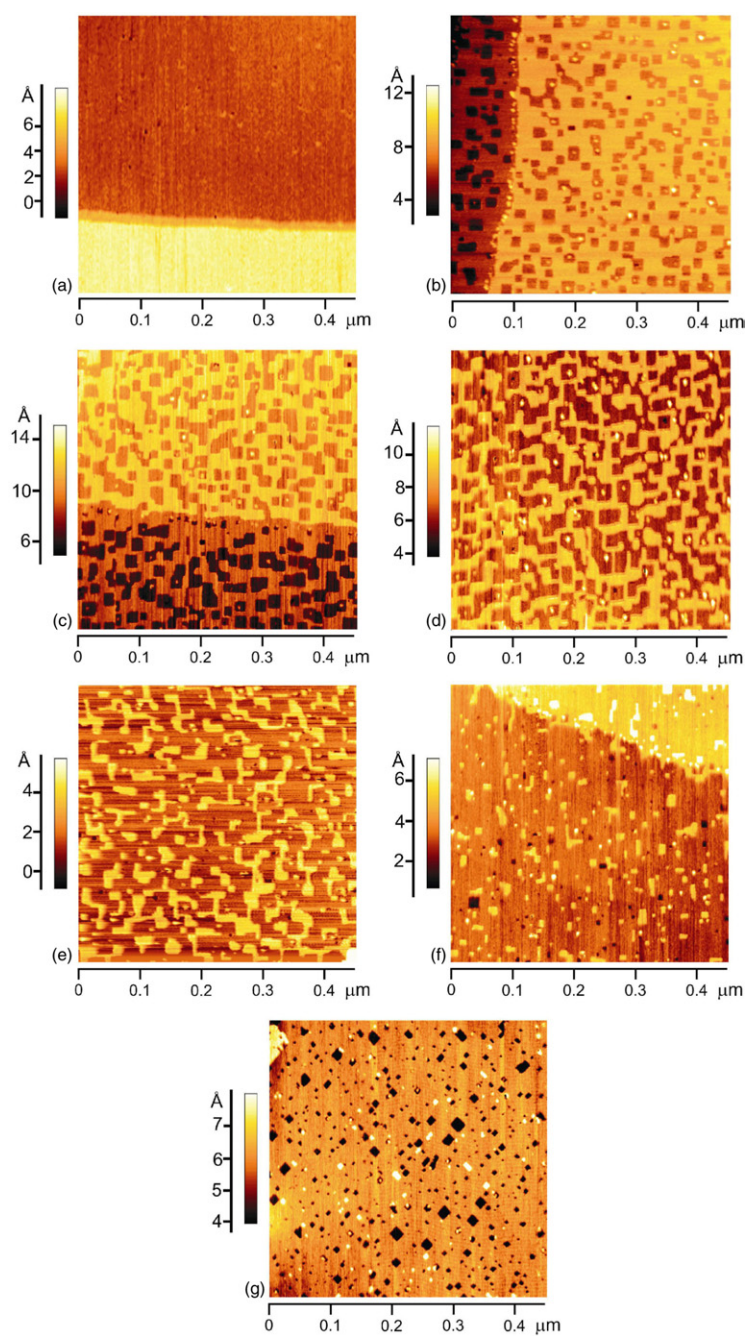


**Figure 3.** Series of NC-AFM images illustrating evolution of the RbI(001) surface irradiated with UV light ( $\lambda \leq 200$  nm) at sample temperature  $100^\circ\text{C}$ . The sequence starts from a virgin surface (a) and continues with gradually increasing photon dose corresponding to the yield oscillations from figure 4: image (d) corresponds to the yield maximum of the first cycle; image (f) corresponds to the yield minimum after the first cycle; images (b), (c), and (e) correspond to intermediate irradiation times. Image (g) represents the second cycle of RbI surface evolution—the first topmost plane is almost totally desorbed and the pits are grown in the next atomic plane.

(This figure is in colour only in the electronic version)



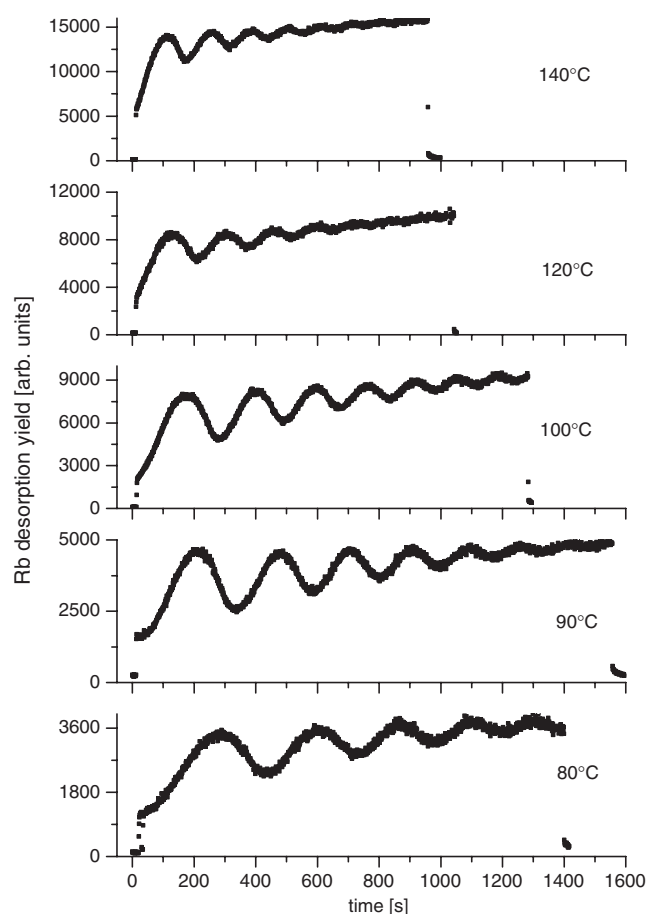


**Figure 4.** UV-photon stimulated desorption of RbI(001). A set of Rb yield oscillations obtained for various temperatures of the sample.

area. In our UV-experiments such absolute evaluation was not possible but the relative yield could easily be estimated and used for studying the temperature dependence of the desorption yield. Such analysis has been performed for each of the yield dependences from figure 4. The results are shown in figure 6, where the dependence of the logarithm of the inverse period (which is proportional to the efficiency of desorption) on the inverse of the sample temperature is shown. The dependence can be fitted accurately by a straight line. The slope of the line corresponds to an activation energy of  $0.17 \pm 0.01$  eV.

#### 4. Desorption due to band-to-band excitations

The yield spectral dependence at excitation energies corresponding to band-to-band transitions reflects both the varying efficiency of the desorption process and the structure of the reflectivity function describing the fact that a significant fraction of the primary photons is reflected from the surface. As demonstrated in figure 1, the maxima in the surface reflectivity spectrum are correlated with intensity drops in the desorption yield. Taking into account that for the given

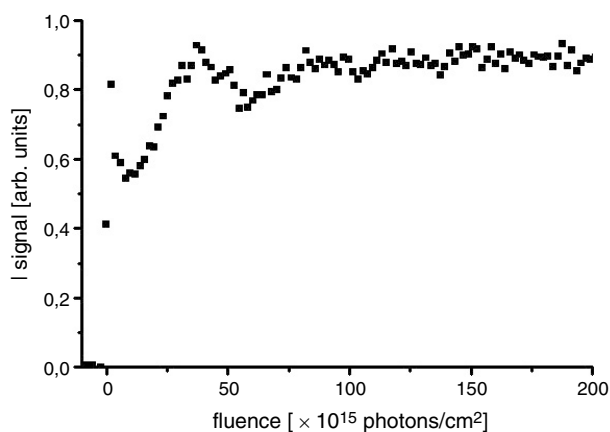


**Figure 5.** I atom desorption yield as a function of the UV-laser irradiation time. The UV-laser energy was 5.8 eV.

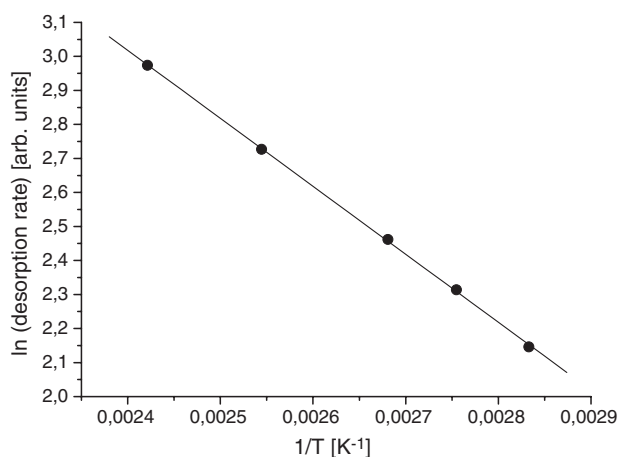


**Figure 6.** Arrhenius plot of the temperature dependence of Rb atoms emitted from a RbI(001) crystal with UV photons.

circumstances the absolute value of the reflectivity could approach 30% [20], a reasonable correspondence is seen between both the reflectivity and the yield curves.

When an electron or a photon with energy higher than the bandgap energy (of the order of 10 eV for halides) reaches the alkali halide crystal, it causes creation of hot electron-hole pairs by inelastic interactions with the crystal lattice [2, 7, 29, 30]. As mentioned in section 3, the penetration depth of 10 eV photons in alkali halides is quite substantial and in fact comparable to the depth of 1 keV electrons [27, 28, 31]. The electrons and holes could efficiently migrate to the surface via uncorrelated diffusion of the conduction band electron and the hole having an excess of kinetic energy (hot hole [29, 30]). The surface recombination of the pair occurs with prompt emission of non-thermal halogen and creation of the surface F-centre [2, 13]. This process has been proposed for the first time by Li *et al* [32] for explanation of photon-stimulated ejection of halogen atoms from alkali halide nanocrystals. Later Puchin *et al* [33]

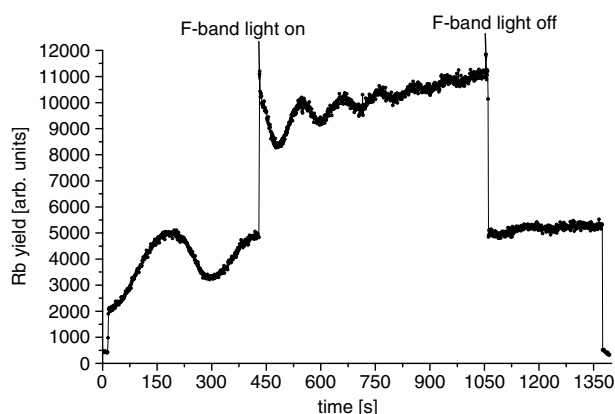


**Figure 7.** Dependence of Rb desorption signal on time of UV-photon irradiation for RbI(001) surface and simultaneous co-excitation by F-band light (reproduced from [23]).

have confirmed theoretically such a process for (100) surface of NaCl. Alternatively, the electron–hole pair could self-trap, leading to production of the Frenkel pairs (so called F-centre and H-centre pair of defects) [3, 4]. Diffusion of these defects in the vicinity of the surface can lead to thermal desorption of crystal constituents. An H-centre migrating to the surface produces a halogen adatom [34]. Since the binding energy of such an atom is relatively low (0.14 eV—[33]), it leaves the surface easily even at room temperature. The behaviour of an F-centre in the vicinity of the crystal surface is less known. In fact, during electron irradiation of alkali halides (NaCl(100) crystal, [35]) F-centres in the ground state are accumulated under the crystal surface. Saalminen *et al* [36] have demonstrated that ground state F-centres in the bulk of the alkali halides are immobile, but those excited (by light or by irradiating electron beam) become highly mobile. Therefore, illumination of the electron pre-irradiated crystal with light at a wavelength corresponding to the F-centre absorption band [35] drives the accumulated F-centres to the surface and causes desorption of alkali atoms.

The theoretical adiabatic potential energy surface (APES) calculations by Puchin *et al* [37] have shown that an F-centre in the ground state cannot initiate desorption because of an energy deficit of about 2 eV. Furthermore, a 2p-excited F-centre could have sufficient energy to desorb an atom but there is an energy barrier which inhibits the desorption [37]. Desorption is more probable, however, from low-coordinated surface lattice sites like steps, kinks and corners. The accumulation of ground-state F-centres together with the preferential desorption from low-coordinated sites on the surface plays a crucial role in explanation of the desorption yield oscillations as a function of the absorbed dose of electrons [24, 37, 38].

## 5. Co-excitation with visible light

In order to understand the role of electronic excitation of the F-centres in photon stimulated desorption better, a series of PSD experiments with simultaneous excitation by UV and visible light has been performed. In figure 7 the yield of Rb atoms emitted from the RbI surface at initial stages of UV-photon irradiation is presented. After removal of 1.5 ML (i.e. in the maximum of the second cycle of oscillations of the yield) the visible light was turned on. As a result, an instant desorption signal increase is recorded, as well as decrease of the period of oscillatory dependence. Both these effects occur as a result of considerable increase of the

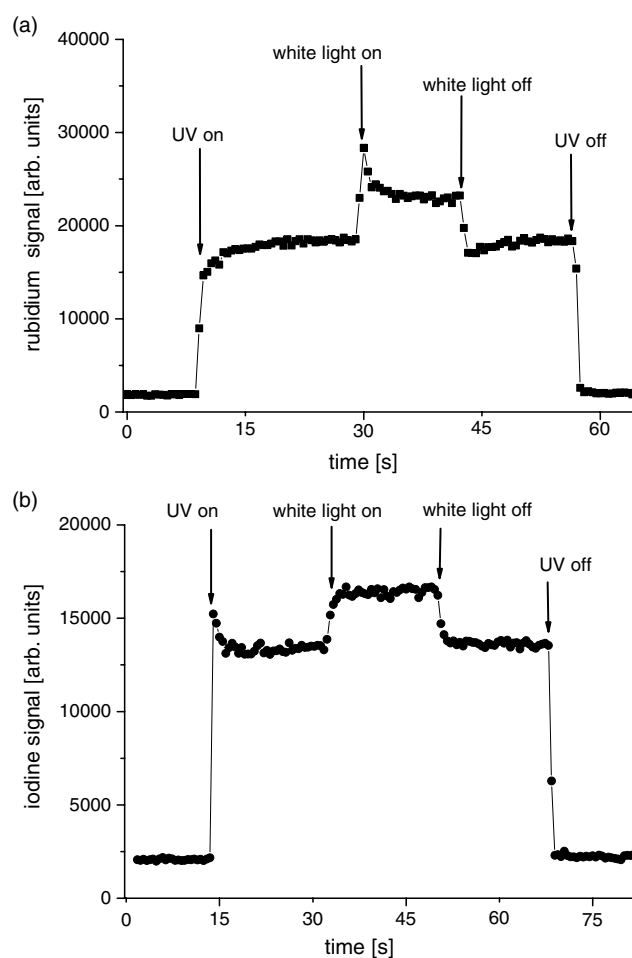


**Figure 8.** Relative changes of Rb (a) and I (b) quadrupole mass spectrometer signals for a prolonged UV-photon irradiation of the RbI(001) surface with and without simultaneous co-excitation by F-band light. The moments of turning on and off F-band light are shown by arrows. The surface temperature was 180 °C.

desorption yield. In figure 8 the changes in partial desorption yields caused by co-excitation are compared for Rb and I atoms (figures 8(a) and (b) respectively). At these experiments the yields are measured for UV-photon doses sufficiently large to obtain saturation of the signals, i.e. when the yield oscillations vanish. It is clear that additional illumination of the sample with light causes significant increase of the desorption yield for both halogen and alkali atoms. Although the magnitude of the signal increase is similar for both components, there are important differences in the character of ‘light-on’ and ‘light-off’ changes of the signals. Whereas Rb yield rises sharply at first and then decreases to almost half of the initial increase, the I signal is rising more slowly, approaching the saturation value only after several seconds of irradiation. Switching off the visible light causes a rapid fall of the Rb signal followed by some increase into a saturation level and slower decrease of the I signal. The same behaviour has been observed for light co-excitation in electron stimulated desorption [39]. Using a set of interference filters it was possible to measure a relative yield enhancement as a function

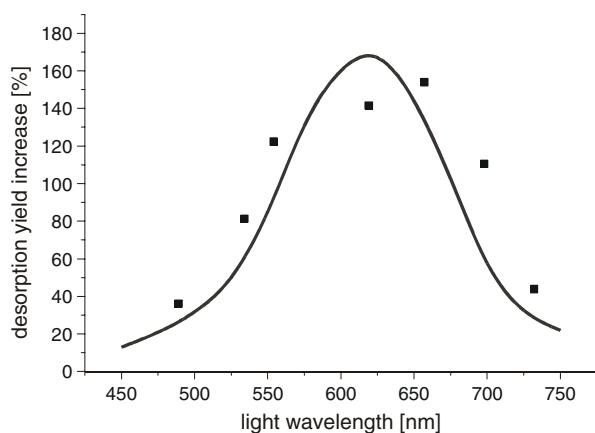


**Figure 9.** Spectral dependence of the relative K desorption yield increase induced by visible light illumination of the electron bombarded KBr crystal. The solid line is drawn to guide the eye and represents the optical absorption profile of KBr F-centres taken from [36].

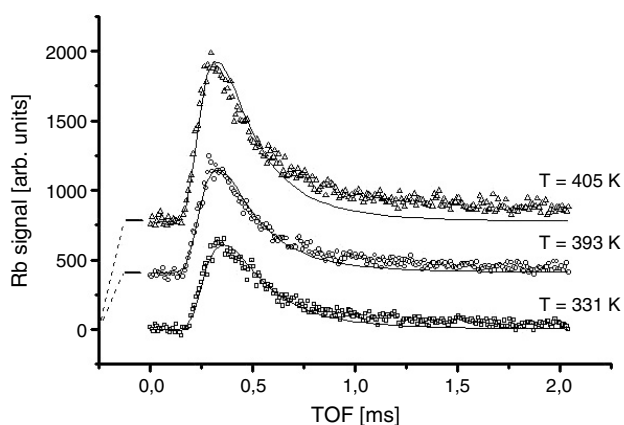


**Figure 10.** Time-of-flight distributions of Rb atoms desorbed from RbI(001) crystal due to co-citation with UV photons and 532 nm laser pulses. Solid lines represent the theoretical curves, i.e. Maxwell–Boltzmann distributions, with the macroscopic surface temperatures measured with a thermocouple and denoted in the figure.

of the wavelength of the visible light. The example of such a dependence obtained for the KBr crystal is reproduced in figure 9. It is seen that the yield enhancement curve follows the F-centre absorption function for this crystal. This clearly indicates that the 2p excited F-centres are significantly more mobile than the ground state ones and this enhanced mobility facilitates the emission of both desorption components. Although it is likely that the excited F-centre arriving at the surface can cause neutralization of surface alkali ion, which then could evaporate thermally, the enhancement of the halogen component requires more consideration. Apparently, the enhanced emission of alkalis at the expense of the stable ground state F-centre concentration is linked to the increase of the halogen signal. In a steady state, the H-centre diffusion takes place in a lattice containing a number of ground state F-centres which can act as annihilation traps. Furthermore, the concentration of stable F-centres is controlled by the

surface topography (see the previous section). As a result of F-centre and H-centre annihilation the thermal halogen signal should vary with the irradiation dose, 'sensing' the inverse F-centre concentration at surface proximity. Such behaviour has been demonstrated by Such *et al* [24] for electron stimulated desorption.

We have studied the effect of visible light co-excitation on the efficiency of the PSD process in more detail by means of a mass selected time-of-flight spectroscopy stimulated by second harmonic pulses of a Nd,YAG laser. In that experiment a RbI crystal was desorbed with UV photons from the deuterium lamp. In addition, the surface was illuminated with 532 nm photon pulses of approximately 10 ns in duration with the repetition frequency of 50 Hz. The energy of the pulses is located within the tail of the F-centre absorption band for RbI. Therefore, any effect of the F-centre excitation on the efficiency of the PSD process should result in appearance of the correlated peak in the appropriate part of the mass spectrum of desorbed particles. Such time-of-flight distributions obtained for rubidium atoms desorbing from the RbI crystal at three different surface temperatures are presented in figure 10. The solid lines in the figure represent Maxwellian distributions of translational energies calculated for experimental values of the sample temperature as measured with a thermocouple. It is seen that the calculated curves describe well the experimental dependences except for a low energy tail of the distribution obtained for the highest temperature. This discrepancy indicates that a fraction of desorbed Rb atoms is emitted with delays of the order of a millisecond. We believe that such a delay reflects the fact that F-centres from deeper layers could arrive at the surface due to diffusion of the excited F-centres at elevated temperatures [26]. In order to understand the nature of F-centre diffusion one has to remember that the 2p excited state of the F-centre is located within the unoccupied states of the conduction band of the crystal. Therefore, it is likely that the lifetime of such an excited F-centre is rather short. On the other hand, the 2p excited centre might be considered as equivalent to an electron in the conduction band and a halogen vacancy which undergo uncorrelated migration in the crystal.

The halogen component of desorption is enhanced due to light illumination but laser pulses do not generate any correlated halogen emission which could be seen in a time-of-flight spectrum. Apparently, the transient change of F-centre concentration in the surface layers, possibly induced by a single laser pulse, is too small to change significantly the H and F centre recombination probability. This hypothesis is supported by the observation that the characteristic time for rise and decay of the I signal in a co-excitation experiment (see figure 8(b)) is of the order of seconds, i.e. it is a few orders of magnitude too slow to be seen in the timescale of our time-of-flight measurements (milliseconds). However, permanent illumination with visible light is causing a significant change of accumulated concentration of F-centres in the sub-surface region and it is causing visible reduction of the H-centres arriving at the surface due to possible H-F pair recombination (figure 8(b)). Such an explanation is strongly supported by the results of time-of-flight distribution measurements performed under continuous illumination of the sample with visible light (see figures 2(a) and (b)). In that last case, the time-of-flight spectra are triggered by UV-light pulses (deuterium lamp) from the mechanical chopper. It is seen that all visible light enhancement of the iodine signal (figure 2(a)) is due to thermal emission, i.e. due to increased probability of H-centres for arriving at the surface and causing desorption of thermal halogen. Under 'visible light-on' circumstances almost all F-centres created by a single UV pulse are subsequently excited and transported into the surface resulting in Rb desorption. Such increased mobility of excited F-centres minimizes the concentration of stable, ground state F-centres which could act as H-centre annihilation traps. It is interesting to note that the shape of the Rb time-of-flight spectrum (figure 2(b)) remains unchanged under the white light illumination, whereas its amplitude is reduced in comparison to 'light-off' distribution. It is plausible to assume that the effective



timescale for F-centre migration is longer than 1 ms. Therefore, a large fraction of F-centres created by a single UV pulse is emitted with a considerable delay and consequently it could not be accounted for in the displayed part of the distribution (flight times below 1 ms). On the other hand, the Rb signal integrated over time is enhanced by the light illumination as seen in figure 8(a).

## 6. Concluding remarks

Non-contact atomic force microscopy and mass selected time-of-flight spectroscopy have been used for studying atomization of an alkali halide crystal due to UV-photon induced desorption of surface constituents. The investigations resulted in a number of conclusive findings, allowing for better understanding of the desorption mechanism.

Primary excitation at threshold energies leads to creation of localized excitations in the vicinity of the surface, either in the form of surface or bulk fundamental excitons, depending on the available photon energy and the electronic structure of the sample. Direct formation of the surface excitons leads to prompt emission of non-thermal halogen leaving behind an F-centre localized at the surface site. Bulk fundamental excitons either migrate to the surface and cause halogen desorption as above, or they thermalize by interacting with the lattice to form a localized defect, i.e. a self-trapped exciton. Non-radiative decay of the self-trapped exciton leads to formation of a pair of point defects: F- and H-centres.

The H-centre (which represents a form of interstitial halogen atom) could easily migrate to the surface and evaporate thermally. This is the source of thermal halogen emission. Accumulation of F-centres in the subsurface layers could trap and annihilate the migrating H-centres, leading to a considerable reduction of the thermal halogen emission.

Our results demonstrate that F-centres play a crucial role in the process. Although the ground-state F-centre is immobile, its excitation either by the primary beam itself, or by illumination with light within the absorption F-band, provides a vacancy transport from the bulk to the surface and detailed balancing of the desorption of halogen atoms and the desorption of alkali atoms.

Photons with energy higher than the bandgap energy cause creation of hot electron-hole pairs due to inelastic inter-band transitions. The electrons and holes could efficiently migrate to the surface due to an excess of kinetic energy (hot hole). The surface recombination of the pair occurs with prompt emission of non-thermal halogen atoms. Alternatively, the hole can self-trap by interaction with the lattice and regain the electron, transforming into a self-trapped exciton.

We have demonstrated that surface topography modification occurs due to creation of the excitonic states in the crystal bandgap by photon irradiation. Non-contact force microscopy studies reveal that randomly spread rectangular pits of monolayer depth in the topmost layer of the crystal are formed during irradiation. Growth and coalescence of the pits lead to the layer-by-layer desorption mode. It is shown that, similarly to electron stimulated desorption, varying surface topography could affect and modulate periodically the diffusion processes driving photon-induced defects from the bulk of the material towards its surface. Furthermore, simultaneous irradiation of the crystal by UV photons and visible light within the F-centre absorption band increases average F-centre mobility, which has a profound effect on both the morphology of the surface and the desorption process efficiency. Such processes could be applied in controlled surface nanostructuring. In fact, the KBr surface nanostructured by electron stimulated desorption has been used as a template for complex molecule deposition and immobilization [40, 41]. Such structures could be applied as model systems for molecular electronics.

## Acknowledgments

The preparation of this paper was supported by the European Commission, under contract no MTKD-CT-2004-003132, Sixth FP-Marie Curie Host Fellowships for Transfer of Knowledge: 'Nano-Engineering for Expertise and Development-NEED' and by the Polish Ministry of National Education and Research.

The authors are grateful to Professor N H Tolk (Vanderbilt University, Nashville, TN, USA) for providing access to the Vanderbilt UV-laser facility.

## References

- [1] For examples, see Williams E M and Palmer R E (ed) 1997 *Desorption Induced by Electronic Transitions* (New York: Elsevier)
- [2] Szymonski M 1993 *Kgl. Dan. Vid. Selsk., Mat.-Fys. Medd.* **43** 495
- [3] Song K S and Williams R T 1993 *Self-Trapped Excitons* (Berlin: Springer)
- [4] Itoh N and Stoneham A M 2000 *Materials Modification by Electronic Excitation* (Cambridge: Cambridge University Press)
- [5] Overeijnder H, Szymonski M, Haring A and de Vries A E 1978 *Radiat. Eff.* **36** 63
- [6] Overeijnder H, Szymonski M, Haring A and de Vries A E 1978 *Radiat. Eff.* **38** 21
- [7] Szymonski M, Kolodziej J J, Czuba P, Piatkowski P, Poradzisz A, Tolk N H and Fine J 1991 *Phys. Rev. Lett.* **67** 1906
- [8] Hess W P, Joly A G, Gerrity D P, Beck K M, Sushko V P and Shluger A L 2001 *J. Chem. Phys.* **115** 9463
- [9] Hess W P, Joly A G, Gerrity D P, Beck K M, Sushko V P and Shluger A L 2002 *J. Chem. Phys.* **116** 8144
- [10] Henyk M, Joly A G, Beck K M and Hess W P 2003 *Surf. Sci.* **528** 219
- [11] Hess W P, Joly A G, Beck K M, Sushko V P and Shluger A L 2004 *Surf. Sci.* **564** 62
- [12] Beck K M, Joly A G, Dupuis N F, Perozzo P, Hess W P, Sushko V P and Shluger A L 2004 *J. Chem. Phys.* **120** 2456
- [13] Hess W P, Joly A G, Beck K M, Henyk M, Sushko V P, Trevisanutto P E and Shluger A L 2005 *J. Phys. Chem. B* **109** 19563
- [14] Wurz P, Sarnthein J, Husinsky W, Betz G, Nordlander P and Wang Y 1991 *Phys. Rev. B* **43** 6729
- [15] Liu D, Albridge R G, Barnes A V, Bunton P H, Ewig C S, Tolk N H and Szymonski M 1993 *Surf. Sci. Lett.* **281** L353
- [16] Brinciotti A, Zema N and Piacentini M 1991 *Radiat. Eff. Defects Solids* **119-121** 559
- [17] Brinciotti A, Piacentini M and Zema N 1994 *Radiat. Eff. Defects Solids* **128** 559
- [18] Szymonski M, Kolodziej J J, Czuba P, Korecki P, Piatkowski P, Postawa Z, Piacentini M and Zema N 1996 *Surf. Sci.* **363** 229
- [19] Zema N, Piacentini M, Czuba P, Kolodziej J J, Piatkowski P, Postawa Z and Szymonski M 1997 *Phys. Rev.* **55** 5448
- [20] Tomiki T, Miyata T and Tsukamoto H 1973 *J. Phys. Soc. Japan* **35** 495
- [21] Hoeche H, Toennies J P and Vollmer R 1993 *Phys. Rev. Lett.* **71** 1208
- [22] Hoeche H, Toennies J P and Vollmer R 1994 *Phys. Rev. B* **50** 679
- [23] Szymonski M, Struski P, Siegel A, Kolodziej J J, Such B, Piatkowski P, Czuba P and Krok F 2002 *Acta Phys. Pol.* **33** 2237
- [24] Such B, Kolodziej J, Czuba P, Piatkowski P, Struski P, Krok F and Szymonski M 2000 *Phys. Rev. Lett.* **85** 2621
- [25] Szymonski M, Kolodziej J, Such B, Piatkowski P, Struski P, Czuba P and Krok F 2001 *Prog. Surf. Sci.* **67** 123
- [26] Kolodziej J J, Such B, Czuba P, Krok F, Piatkowski P, Struski P, Szymonski M, Bennewitz R and Schaer S 2001 *Surf. Sci.* **482** 903
- [27] Peimann C J and Skibowski M 1971 *Phys. Status Solidi b* **46** 655
- [28] Bronshteyn I M and Protsenko N 1970 *Radio Eng. Electron. Phys.* **15** 677
- [29] Elango M A, Kadchenko V N, Saar A M and Zhurakovski A P 1976 *J. Lumin.* **14** 375
- [30] Elango M A 1994 *Radiat. Eff. Defects Solids* **128** 1
- [31] Al Jammal T, Pooley D and Townsend P D 1973 *J. Phys. C: Solid State Phys.* **6** 247
- [32] Li X, Beck R D and Wetten R L 1992 *Phys. Rev. Lett.* **68** 3420
- [33] Puchin V E, Schluger A L and Itoh N 1993 *Phys. Rev. B* **47** 10760
- [34] Szymonski M 1980 *Radiat. Eff.* **52** 9
- [35] Kubo T, Okano A, Kanasaki J, Ishikawa K, Nakai Y and Itoh N 1994 *Phys. Rev. B* **49** 4931

- 
- [36] Salminen O, Riihola P, Ozols A and Viitala T 1996 *Phys. Rev. B* **53** 6129
- [37] Puchin V, Shluger A, Nakai Y and Itoh N 1994 *Phys. Rev. B* **49** 11364
- [38] Such B, Czuba P, Piatkowski P and Szymonski M 2000 *Surf. Sci.* **451** 203
- [39] Struski P 2002 *PhD Thesis* Jagiellonian University, Cracow (in Polish)
- [40] Nony L, Gnecco E, Alkauskas A, Baratoff A, Bennewitz R, Pfeiffer O, Maier S, Wetzel A, Meyer E and Gerber C 2004 *Nano Lett.* **44** 2185
- [41] Nony L, Bennewitz R, Pfeiffer O, Gnecco E, Meyer E, Eguchi T, Gourdon A and Joachim C 2004 *Nanotechnology* **15** S91